104 (2025) 105231

Contents lists available at ScienceDirect

Poultry Science

journal homepage: www.elsevier.com/locate/psj

Isolation, identification, whole genome sequence analysis, and pathogenicity of a potential recombinant goose parvovirus

Qinghe Zhu, Huinan Li, Hansong Li, Wenfei Bai, Jingxuan Zhou, Ming Liu, Yingying Zhao, Limin Jiang, Ying Sun, Jia Sun, Jingjing Zhao, Jia Hu, Chunqiu Li, Xiaoxu Xing, Dan Yang, Dongbo Sun *

College of Animal Science and Veterinary Medicine, Heilongjiang Bayi Agricultural University, No. 5 Xinfeng Road, Sartu District, Daqing 163319, PR China

ARTICLE INFO

Keywords:
Goose parvovirus
whole-genome sequence
recombination
pathogenicity

ABSTRACT

Goose parvovirus (GPV) is the etiological agent responsible for gosling plague (GP), which is an acute hemorrhagic infectious disease affecting geese, posing significant economic challenges to the poultry industry. Furthermore, recent studies have identified that the novel goose parvovirus (NGPV), a recombinant variant of the classic GPV, is responsible for duck short beak dwarfism syndrome, which has significantly affected duck farm. Therefore, the infection and genetic evolution of GPV have attracted widespread attention of researchers in poultry disease. In order to clarify the prevalence and genetic evolution of clinically severe GPV in the Heilongjiang region, this study successfully isolated a strain of GPV HLJ2023 from goose embryos, which results in the mortality rate of 100 % after 5 generations. The electron microscope shows that the virus particles are spherical, with a diameter of approximately 28 nm, and HLJ2023 strain has a total genome length of 5048 nt. SimPlot analysis showed that HLJ2023 strain is closely related to duck parvovirus and NGPV in the VP3 gene region. Recombination analysis showed that the isolated strain is a potential recombinant of the NGPV JS191021 strain and the GMD (Goose parvovirus hosted by Muscovy duck) PT strain. the strong pathogenicity of HLJ2023 strain to goslings. 36 h after the challenge, the goslings were depressed and had a mortality rate up to 100 %. Autopsy revealed intestinal bleeding, thinning of the intestinal wall, and a large amount of fibrous clots and fragments in the intestinal cavity. This study isolated a highly pathogenic potential recombinant GPV, further expanding the genetic evolution and pathogenicity information of avian parvovirus. At the same time, the isolated strain provides a candidate strain for the development of biological products for treating GPV.

Introduction

Goose parvovirus (GPV) is an acute or subacute sepsis infectious disease that be transmitted in geese and muscovy ducks. It was first discovered in China in 1956 and has since been reported in multiple countries and regions around the world (Liu et al., 2017; Niu, et al., 2018a; Tatar-Kis, et al., 2004). GPV is mainly transmitted through the secretions and excretions of infected geese, causing clinical symptoms such as brain atrophy, weight loss, weakness, and severe diarrhea in geese under 10 days old and muscovy ducks over 2 weeks old, Infected geese exhibit fibrinous and necrotic enteritis, as well as small intestinal embolism, which is formed when the surface of the intestinal mucosa dies and falls off. During epidemic years, the mortality rate exceeds 50 %, causing serious economic losses to the goose breeding industry (He, et al., 2022a; Yin, et al., 2012). However, the continuous mutation of GPV and the delayed update of vaccine strains may affect the preventive effect of the virus. Not only that, a new duck short beaked dwarf syndrome (SBDS) has been identified as the novel goose parvovirus (NGPV) in the waterfowl parvovirus genus, causing beak atrophy, growth retardation, tongue exposure, and osteoporosis in commercial ducks (Kexiang, et al., 2016). Reports showed that the NGPV also derived from the recombination and mutation of GPV(Kexiang, Yu, Xiuli, Ma, Zizhang, Sheng, Lihong, Qi, Cunxia and microbiology, 2016; Liu, et al., 2020b). Therefore, the infection and genetic evolution of GPV have attracted widespread attention of researchers (Huo, et al., 2023; Li, et al., 2021; Wang, et al., 2024, 2019, 2021). This study conducted a systematic research on the isolation and identification, whole genome sequence analysis, recombination analysis, and pathogenicity of the

* Corresponding author.
E-mail address: dongbosun@126.com (D. Sun).

https://doi.org/10.1016/j.psj.2025.105231
Received 19 December 2024; Accepted 28 April 2025
Available online 29 April 2025

GPV from the goose farm in Heilongjiang Province. The study explored the phylogenetic relationship between the isolated strains and the MDPV (Muscovy duck parvovirus), as well as the pathogenicity of the GPV, providing a reference for the detection and evolutionary analysis of genetic information of waterfowl parvovirus, as well as the diagnosis and prevention of this disease.

Materials and methods

Ethics statement

The animal experiments were approved by the Ethical Committee for Animal Experiments of Heilongjiang Bayi Agricultural University (Daqing, China). (approval numbers: DWKJXY2024078).

Sample collection and processing

In July 2023, a disease outbreak occurred at a commercial goose farm in Qiqihar, China, experienced an outbreak of disease and Sanhua geese fell ill, with the clinical manifestations of mental depression, loss of appetite, and death of 12-day-old goslings. Autopsy revealed inflammation and necrosis of the small intestinal mucosa, shedding of the intestinal mucosa, and the presence of pale yellow coagulated cellulose "intestinal plugs" in the intestinal lumen, resulting in a mortality rate of 25 % in goslings. Tissue samples from various organs of deceased goslings with symptoms of intestinal embolism were collected and submitted for laboratory analysis.

Virus isolation and identification

To isolate GPV, the liver, spleen, heart, kidney, and small intestine tissues were homogenized with sterile phosphate-buffered saline (PBS, pH 7.4) to a 20 % suspension (w/v) and centrifuged at 6000 × g, at 4 °C for 20 min at 4 °C. The supernatant was filtered using a syringe-driven filter unit with a pore size of 0.22 μm and the filtrate was inoculated into five 10-day-old goose embryos (Jinpeng Co. Jiangsu, China) (0.25 mL/goose embryos) via the allantoic cavity. Embryos were incubated at 37°C and candled daily. Embryos that have died beyond 24 h and those that have survived for 5 days after inoculation were chilled to 4 °C overnight. The allantoic fluid of dead embryos was collected for the detection of GPV and further passage. For EM, the samples were negatively stained as previously described (Jiang, et al., 2018). The viral suspension was subjected to ul-tracentrifugation at 30,000 × g for 30 min to pellet the viral particles, which were negatively stained with 2 % phosphotungstic acid (pH 7.0). The negatively stained samples were examined using a Hitachi-7650 transmission electron microscope (Hitachi, Ltd., Tokyo, Japan). The isolated GPV was named strain HLJ2023.

PCR and sequencing

The allantoic fluid of dead embryos was centrifuged at 1500 × g for 10 min at 4 °C and the supernatants were transferred to a 1.5 mL tube. DNA extraction was performed as previously described (Qi, et al., 2019). Conventional PCR was carried out using One-step PCR Kit (TaKaRa, Dalian, China) with specific primers (GPV-F 5′-GAGCATCAACTC CCGTATGTCC-3′, GPV-R 5′ – CTACTTCCTGCTCGTCCGTGA-3′) to amplify the partial sequence (640 bp) (Niu, Wang, Wei, Zhang, Yang, Chen, Tang and Diao, 2018a). Primers used to detect other goose viruses (goose astrovirus [GoAstV], tembusu virus [TMUV], and goose paramyxovirus [GPMV]) are listed in Table S1. In addition, the reference primers used to supplement the full-length gene sequence are listed in Table S2 (Liu, et al., 2018).

Next-generation sequencing (NGS)

The allantoic fluid of dead embryos was harvested for extracting viral DNA as previously described. The Illumina sequencing and library construction were performed at the Shanghai Tanpu Biotechnology Co., Ltd (Shanghai, China). Briefly, Viral DNA was fragmented with NEBNext® dsDNA Fragmentase®. DNA fragments were used as input to the NEB "NEBNext® Ultra™ II DNA Library Prep Kit for Illumina®" protocol. An Agilent 2100 Bioanalyzer, with a High Sensitivity DNA Kit was used to quantify the library. The library followed the Illumina protocol "Prepare DNA libraries for sequencing on the NovaSeq 6000″. Paired-end 150 nt reads were generated.

Sequence analysis

The viral open-reading frames (ORFs) prediction, amino acids (aa) translation, sequence alignment and pairwised sequence comparisons were performed using the modules of EditSeq and MegAlign of DNASTAR Lasergene 12 Core Suite (DNASTAR, Inc. Madison, WI, USA). The highest similarities between the studied avian parvovirus genome segment and the published sequences were identified by BLASTN online searching program (http://blast.ncbi.nlm.ni-h.gov/ Blast.cgi). Multiple sequence alignments were performed using the multiple sequence alignment tool in DNAMAN 6.0 software (Lynnon BioSoft, Point-Claire, Quebec, Canada). A similarity plot analysis of the whole genome sequence of HLJ2023 strain identified in this study and other avian parvoviruses strains were performed using the sliding window method as implemented in the SimPlot, v.3.5.1 package.

Phylogenetic analysis

For the phylogenetic analysis, the avian parvoviruses genes reference strains were retrieved from the NCBI nucleotide database as reference sequences (Table S3). These nucleotide sequences were then used to generate a neighbor-joining phylogenetic tree using MEGA 6.06 software (Tamura, et al., 2013). A neighbor-joining phylogenetic tree was constructed using the p-distance model and 1000 bootstrap replicates. The phylogenetic tree was annotated with the Interactive Tree Of Life (iTOL) software (http://itol.embl.de/), an online tool for the display and annotation of phylogenetic trees (Letunic and Bork, 2016).

Recombination analysis of the identified HLJ2023 strain

The HLJ2023 strain in this study and the reference sequences of avian parvoviruses genes from GenBank were used for the recombination analysis. The complete sequences were aligned in the ClustalX program, and then screened for possible recombination using the Recombination Detection Program (RDP) (Martin, et al., 2015), GENECONV (Padidam, et al., 1999), BOOTSCAN (Martin, et al., 2005), MaxChi (Smith, 1992), CHIMAERA (Posada and Crandall, 2001), and SISCAN (Gibbs, et al., 2000) methods embedded in RDP4. Only potential recombination events detected by two or more of the programs coupled with phylogenetic evidence of recombination, were considered significant using the highest acceptable *p*-value cutoff of 0.05.

Pathogenicity assessment of isolated GPV strain in goslings

In order to validate the pathogenicity of isolated GPV HLJ2023 strain, artificial infection experimental was conducted in 12 2-day-old healthy goslings, and they were divided into two groups. Among them, 6 goslings were infected by subcutaneous injection with 0.2 mL of the isolated GPV HLJ2023 strain ($10^{5.25}$ ELD_{50}/0.2 mL); while the other, 6 goslings were inoculated with PBS in the same manner, kept separated from the experimental group as control. The mortality of goslings was monitored daily.

Histopathology: Goslings that succumbed post-inoculation

underwent autopsy, during which tissue samples were collected from the spleen, kidney, ileum, duodenum, jejunum, liver, lung, bursa of Fabricius, and brain for histopathological examination. Tissue specimens were fixed in 10 % formalin for 72 h at ambient temperature, subsequently processed through standard protocols, embedded in paraffin wax, and sectioned into 5 μm slices. These sections were stained with hematoxylin and eosin (HE) and analyzed using light microscopy.

Detection of Viral Loads: Equal quantities (1 g) of tissue samples were homogenized in 5 mL of PBS. After centrifugation at 4200 × g for 10 min at 4 °C, the supernatant was used for DNA extraction, which were performed according to the protocols described by Qi et al. (Qi, Su, Guo, Li, Wei, Feng and Sun, 2019). The quantitative PCR (qPCR) performed with primers targeting VP3 (forward: 5′- TCCCGTCGGATGTCTATG-3′, reverse: 5′ – GCTACTGCCTGTCCTTCA-3′) (Dong, 2011). Standard plasmids were constructed for use in the present study. The qPCR was performed with SYBR Green I fluorescent dye and the QuantStudio™ 3 Real-Time PCR System (Applied Biosystems, Carlsbad, CA, USA). For qPCR, each 20 μL reaction included 10 μL of 2 × SYBR® Premix Ex Taq polymerase (Takara Bio, Inc.), 2 μL of DNA, and 0.25 μM of each primer. The thermal cycling conditions were: denaturation at 95 °Cfor 30 s, followed by 40 cycles of 95 °Cfor 25 s and 60 °Cfor 60 s. Ten-fold dilutions of the standard plasmid (10^{10}-10°) and the negative control (distilled water) were included in each plate. Each sample was assayed three times. The quantity of GPV viral DNA was calculated based on the results for the standard plasmid.

Statistical analysis

Each experiment was repeated independently three times and average values were taken. No data were excluded in this study. All data were presented as means ± standard deviations and were analyzed using the one-way analysis of variance (ANOVA) procedure in GraphPad Prism 7.0 (GraphPad Software Inc., San Diego, CA, USA). Statistical significance was set at $P < 0.05$.

Results

Virus isolation and identification

To isolate the HLJ2023 strain, tissue homogenates from GPV-positive samples were inoculated into goose embryos. By the fifth passage, the inoculation resulted in 100 % mortality of the goose embryos within five days post-inoculation (dpi). Gene-specific PCR analysis confirmed the presence of GPV in the allantoic fluid of the deceased embryos (Fig. 1**A**). Electron microscopy examination revealed that the purified virus particles were spherical with an approximate diameter of 28 nm (Fig. 1**B**).

Genome sequence analysis

The complete genome sequence of strain GPV HLJ2023 have been deposited in GenBank (GenBank accession no. PQ206310), containing two main open reading frames (ORFs). The length of the left ORF is 1884 nt, encoding a non-structural protein required for the regulation of capsid gene expression composed of 627 amino acids. The length of the ORF on the right is 2199 nt, encoding three structural proteins composed of 732 amino acids. Three structural proteins share a common C-terminal region. The gene lengths encoding VP1, VP2, and VP3 proteins are 2199 nt, 1764 nt, and 1605 nt, respectively (Fig. 2).

SimPlot analysis showed that the complete genome sequence of the HLJ2023 strain isolated in this study was highly similar to classical GPV, but was highly similar to Muscovy duck parvovirus and GMD in the nucleotide region of VP3 gene 3519-4219. Further homology analysis showed that the homology of the whole genome sequence of the isolated strain with GPV, NGPV, MDPV, and GMD was 78.7-99.9 %, 78.3-99.9 %, 70.2-85.1 %, and 73.0-97.7 %, respectively. In the nucleotide region of 3519-4219, the homologyof isolated strain HLJ2023 with MDPV and GMD was 94.7-99.9 % and 77.9 %−98.9 %, respectively (Fig. 2). Further regional homology analysis showed that the homology between the isolated strain HLJ2023 and non-structural proteins NSP1, NSP2, and structural proteins VP1, VP2, and VP3 genes of classical GPV was 83.2-100 %, 81.3-100 %, 90.0-99.8 %, 91.7-99.9 %, and 94.0-99.9 %, respectively. The homology with the NGPV was 83.0-99.8 %, 81.2-99.9 %, 84.0-99.7 %, 84.4-99.8 %, and 86.0-99.8 %, respectively. The homology with MDPV was 82.4-83.3 %, 80.6-81.4 %, 80.4-90.1 %, 79.8-91.8 %, and 80.9-94.1 %, respectively. The homology with GMD was 83.0-99.6 %, 81.3-99.6 %, 90.3-98.6 %, 92.0-98.4 %, 94.3-98.3 %, respectively (Table 1).

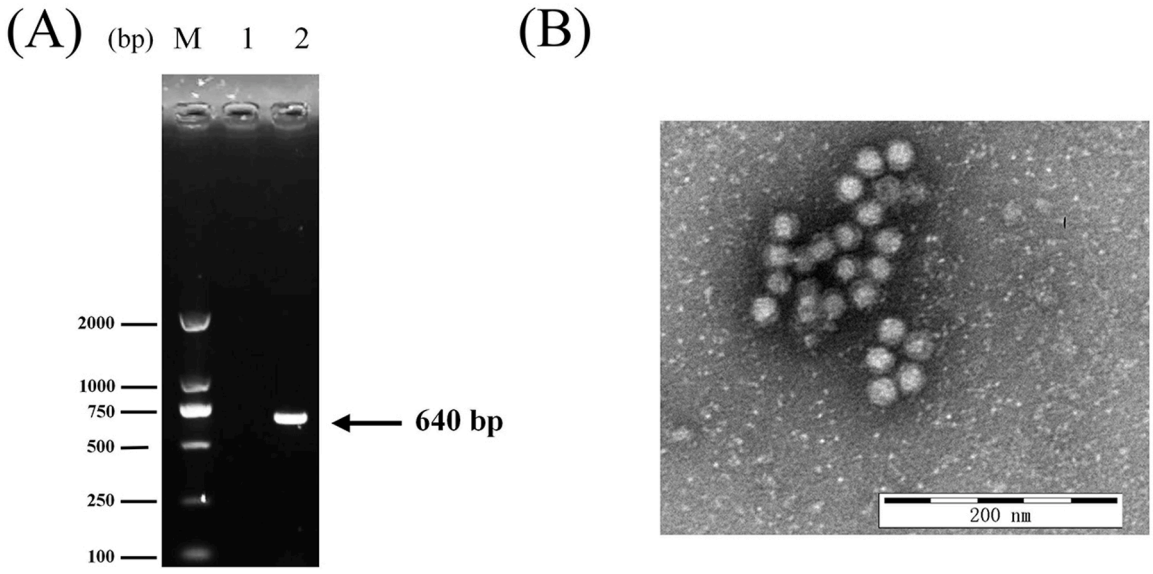

Fig. 1. Identification of isolated GPV strain HLJ2023 with PCR and electron microscopy. (A) PCR. The extracted DNA was analyzed via PCR using GPV specific primers. Note: DNA was extracted from the allantoic fluid of normal goose embryos (1) and from goose embryos inoculated with the GPV positive sample tissue homogenates (2). (B) Electron microscopy of allantoic fluid containing strain HLJ2023 after negative staining with phosphotungstic acid (Scale bar = 200 nm).

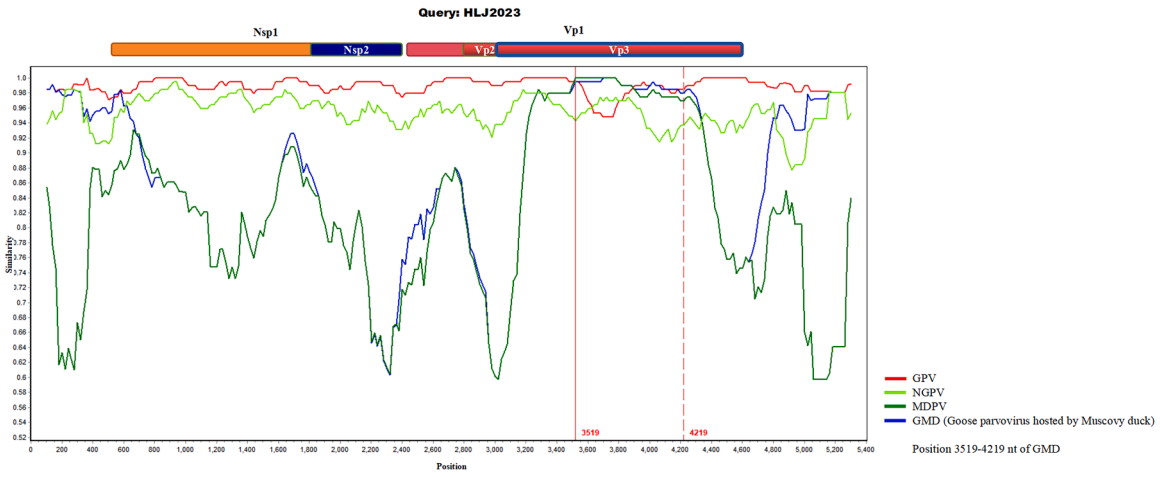

Fig. 2. Similarity plot of the GPV nucleotide sequences of the HLJ 2023 strains identified in this study and the avian parvovirus reference strains, respectively. Note. The HLJ2023 strains identified in our study were set as query strains.

Table 1
Sequence identities between the GPV HLJ2023 strain and the avian parvovirus reference strains.

Virus	Nucleotide identity (%)					
	Genome	NSP1	NSP2	VP1	VP2	VP3
GPV	78.7-99.9	83.2-100	81.3-100	90.0-99.8	91.7-99.9	94.0-99.9
NGPV	78.3-99.9	83.0-99.8	81.2-99.9	84.0-99.7	84.4-99.8	86.0-99.8
MDPV	70.2-85.1	82.4-83.3	80.6-81.4	80.4-90.1	79.8-91.8	80.9-94.1
GMD	73.0-97.7	83.0-99.6	81.3-99.6	90.3-98.6	92.0-98.4	94.3-98.3

Phylogenetic analyses of HLJ2023 strain

The evolutionary relationships between the HLJ2023 strain and other avian parvoviruses were confirmed using the neighbour-joining phylogenetic analysis. By aligning the nt sequences of complete genome and VP3 gene, the phylogenetic trees were finally generated (Fig. 3). The phylogenetic tree analysis based on whole genome sequence shows that MDPV is an independent branch, while GPV is mainly divided into three groups. GI and GII groups are mainly classical GPV, while GIII group is NGPV. The isolated HLJ2023 strain in this study is located in GI group, but its genetic evolution relationship is close to that of the SQ0412 strain of NGPV (Fig. 3**A**). The phylogenetic tree analysis based on the VP3 gene showed similar results. GPV is mainly divided into three groups (GI, GII and GIII). The HLJ2023 strain identified in this study is located in the GI group and is closely related to the genetic evolution of the classical GPV RC70 strain and the NGPV AHAU41 strain. (Fig. 3**B**).

Recombination analysis of HLJ2023 strain

The whole genome sequence of HLJ2023 strain and other avian parvovirus from GenBank were used for the recombination analysis, sequence alignment was carried out through ClustalX program, and detection and analysis were carried out by Recombination Detection

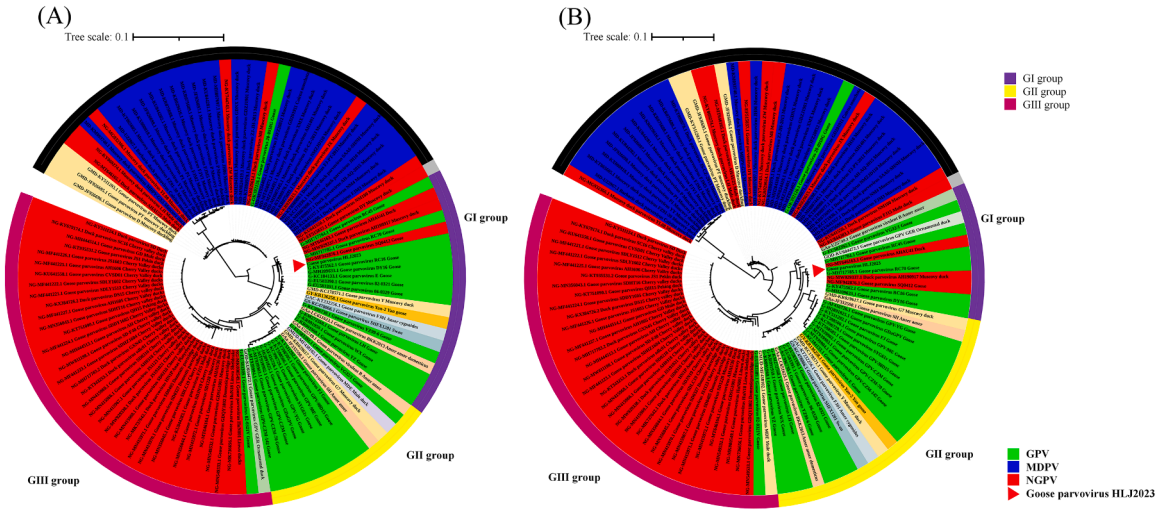

Fig. 3. Phylogenetic analysis of GPV strains. (A) Phylogenetic analysis of GPV strains based on the whole-genome sequence. (B) Phylogenetic analysis of GPV strains based on the VP3 gene sequence. Note. The phylogenetic trees were generated using the neighbor-joining method of MEGA 6.0 with 1000 bootstrap replicates. Source: (G-Goose parvovirus, MD-Muscovy duck parvovirus, NG-Novel goose parvovirus, GMD-Goose parvovirus hosted by Muscovy duck, GAC-Goose parvovirus hosted by Anser cygnoide, GS-Goose parvovirus hosted by Swan, GAa, Goose parvovirus hosted by Anser anser, GMUD-Goose parvovirus hosted by Mule duck, GOD-Goose parvovirus hosted by Ornamental duck), the GenBank accession number, strain name, and host are indicated. (For interpretation of the references to color in this figure legend, the reader is referred to the web version of this article).

Program (RDP) (Martin, Murrell, Golden, Khoosal and Muhire, 2015), GENECONV (Padidam, Sawyer and Fauquet, 1999), BOOTSCAN (Martin, Posada, Crandall and Williamson, 2005), MaxChi (Smith, 1992), CHIMAERA (Posada and Crandall, 2001), and SISCAN (Gibbs, Armstrong and Gibbs, 2000) methods embedded in RDP4. The results show that the breakpoint positions of the recombination event are presented in Table S4. A recombination event that occurred between the NGPV JS191021 strain and the GMD PT strain led to the generation of the potential recombinant HLJ2023 strain. The SimPlot of the recombination event is presented in Fig. 4**A**, in which the NGPV JS191021 strain and the GMD PT strains were used as the major parent strain and minor parent strain, respectively. The recombination event was confirmed by the fast neighbor-joining trees that were constructed using the regions derived from the minor parent strain (4378-3255) (Fig. 4**B**), the ignoring-recombinant region (Fig. 4**C**), and the recombinant region (3255-4378) (Fig. 4**D**).

Pathogenicity analysis of GPV HLJ2023

Clinical signs and gross lesions: Goslings in the GPV HLJ2023 infection group began to show depression at 36 hpi, and began to die at 48 hpi. The mortality rate at 72 hpi reached 100 % (6/6). Survival curves were drawn for the goslings with the Prism 7 program (GraphPad) (Fig. 5**A**). During the autopsy, it was observed that the entire intestinal mucosa became inflamed with diffuse edema. The middle and posterior segments of the intestine become larger, and the intestinal wall becomes thinner. There are numerous fibrous clots and fragments in the intestinal cavity, but solid embolism has not yet formed (Fig. 5**B**). The control group of goslings did not show any mortality or any clinical symptoms.

Histopathology of different tissues: Histopathological analysis showed that the spleen, kidney, liver, lungs, and small intestine tissues of the infected group exhibited significant histopathological changes at 72 hpi (Fig. 6). The overall structure of the spleen tissue is abnormal, and the the lymphatic sheath structure of the splenic white pulp of the spleen has disintegrated, with lymphocyte necrosis and nuclear atrophy visible inside (black arrow) (Fig. 6**j**); Local glomerular vascular loop structure degeneration and necrosis, with loose and disordered structure (black arrow); Localized degeneration and necrosis of renal tubular epithelial cells, damage to luminal structure (red arrow); A small amount of lymphocyte infiltration can be seen locally (yellow arrow) (Fig. 6**k**); Degeneration and necrosis of columnar epithelial cells in the upper layer of ileum mucosa, with structural loss (black arrow) (Fig. 6**l**); Abnormal overall structure of duodenum and jejunum, with loose and disordered mucosal layer structure; The columnar epithelium and intestinal glands were completely replaced by residual protein cellulose (black arrow) (Fig. 6**m, n**); Fatty degeneration of liver tissue, with numerous vacuoles of lipid droplets of different sizes visible in the cytoplasm (black arrow); Localized hepatic sinuses show dilation and hyperemia (red arrow) (Fig. 6**o**); Degeneration and necrosis of alveolar epithelial cells in lung tissue, with visible destruction of alveolar structure and edema (black arrow); Obvious inflammatory cell infiltration in the stroma (red arrow); Localized pulmonary hyperemia (yellow arrow) (Fig. 6**p**); Degeneration, necrosis and shedding of columnar epithelial cells in the upper layer of bursa of fabricius mucosa (black arrow); Disordered structure of cortex and medulla of internal lymph nodes, disappeared structure of lymph follicles, accompanied by localized lymphocyte necrosis, nuclear atrophy and lysis (red arrow) (Fig. 6**q**); Slight edema and loose structure of brain parenchyma in brain tissue (black arrow); Watery degeneration, loose cytoplasm and vacuoles in microglia (red arrow) (Fig. 6**r**).

Measurement of viral load in tissues: The viral loads in the different tissues of the goslings were measured with qPCR (Fig. 7). Viral DNA was

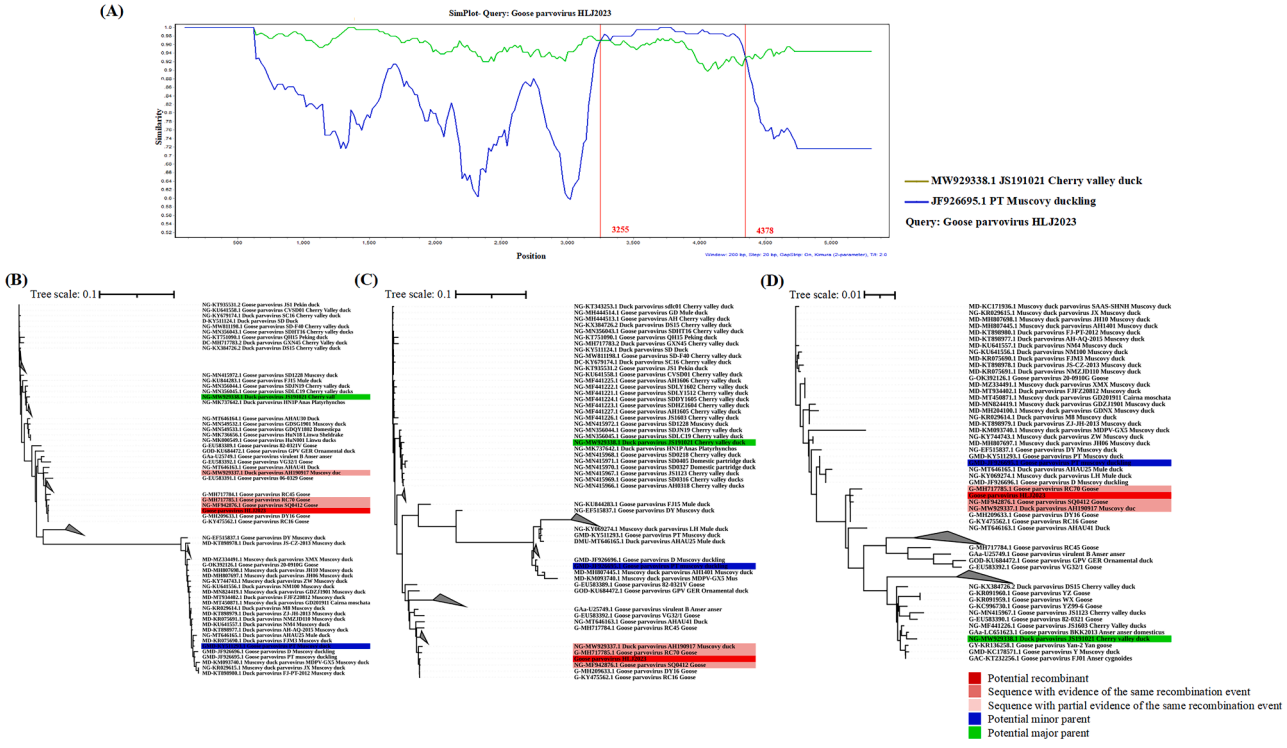

Fig. 4. Identification of recombination events between the major parent strain, JS191021 (green), and the minor parent strain, PT (blue), which led to the potential recombinant HLJ2023 strain (red). (A) SimPlot evidence for the recombination origin based on the pairwise distance, modeled with a window size of 200, step size of 20, and 100 bootstrap replicates. (B–D) A fast neighbor-joining (NJ) tree (1000 replicates, Kimura two-parameter distance) was constructed using the regions derived from the minor parent strain (4379-3254) (B), the ignoring–recombinant region (C), and recombination region (3255-4378) (D). Note. The potential recombination event was detected using RDP (p = 3.334E-14), GENECONV (p = 2.099E-10), Bootscan (p = 1.277E-14), MaxChi (p = 7.839E-07), Chimaera (p = 2.033E-07), SiSscan (p = 1.529E-23), 3Seq (p = 4.058E-07) methods.

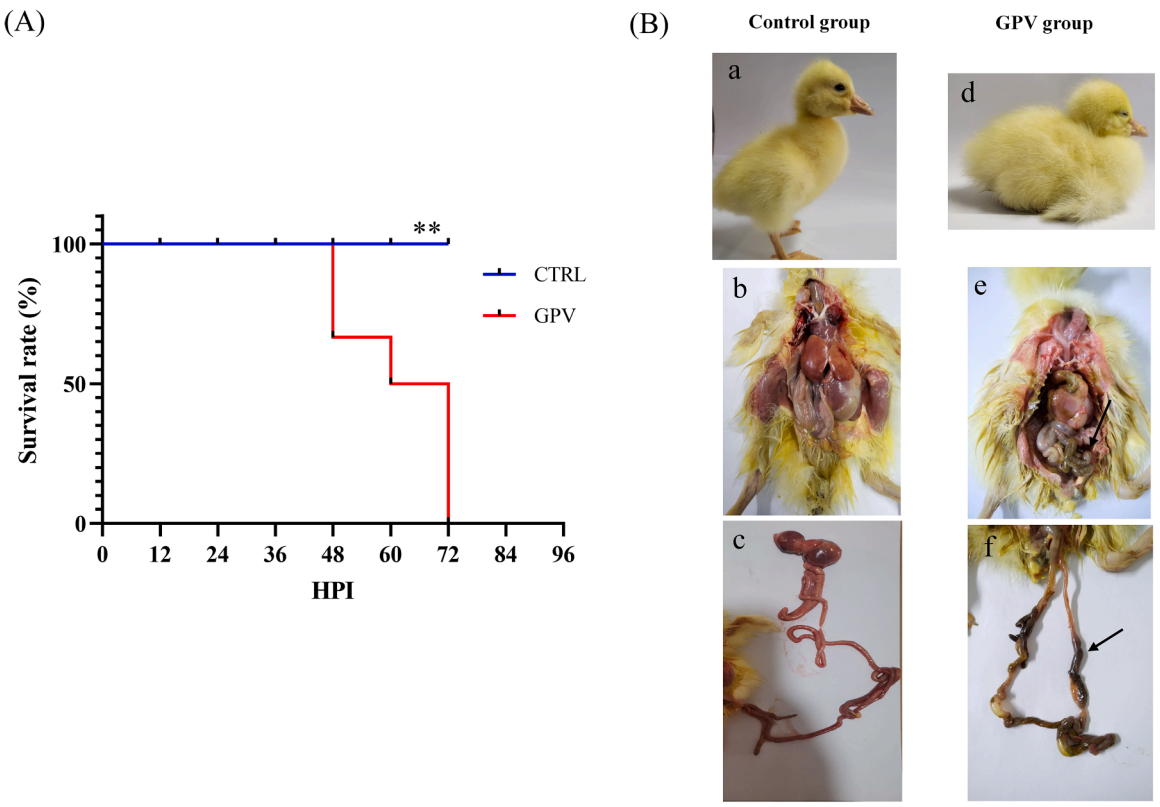

Fig. 5. Survival rates and postmortem lesions of goslings after inoculation with strain HLJ2023. (A) Survival rates of goslings after inoculation with strain HLJ2023. The percentage of goslings that survived in the infected groups was extremely significantly lower than that in the control group. Note: ** indicates that the difference between the infection group and control group was extremely significant. (B) Postmortem lesions in goslings that died at 72 hpi. The infected group of goslings displayed signs of depression (B, d). The middle and posterior segments of the intestine become larger, and the intestinal wall became thinner (B, e). There are a significant amount of blood clots and exudate in the small intestine of infected goslings (B, f). Non-infected control goslings are shown in a, b, and c.

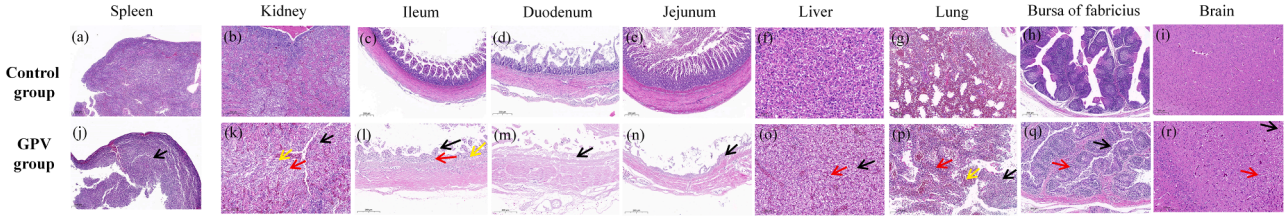

Fig. 6. Histopathological lesions in tissues from GPV-infected goslings at 72 hpi. (a-i) Histopathology of spleen, kidney, ileum, duodenum, jejunum, liver, lung, bursa of fabricius, and brain tissues in uninfected control group goslings, (j-r) Histopathological changes in spleen, kidney, ileum, duodenum, jejunum, liver, lung, bursa of fabricius, and brain tissues of GPV-infected group goslings.

detected in the spleen (7.76×10^{10} DNA copies/g), Kidney (3.15×10^{10} DNA copies/g), ileum (1.36×10^{10} DNA copies/g), cecum (4.66×10^{9} DNA copies/g), duodenum (3.92×10^{9} DNA copies/g), liver (3.59×10^{9} DNA copies/g), lung (3.83×10^{9} DNA copies/g), rectum (2.44×10^{9} DNA copies/g), jejunum (1.36×10^{9} DNA copies/g), bursa of fabricius (2.06×10^{8} DNA copies/g), brain (2.83×10^{7} DNA copies/g), and heart (4.25×10^{7} DNA copies/g) in the infection group. It should be noted that the number of viral copies were significantly higher in the spleen, kidney, and ileum than in the other tissues.

Discusstion

Since 1956, Goose Parvovirus (GPV) has been extensively disseminated across Europe, the Americas, and Asia. It exhibits high pathogenicity and lethality in geese and ducks, leading to significant economic losses within the poultry industry (Irvine, et al., 2008; Kardogan, et al., 2020). Recent studies have indicated that co-infection with GPV and Goose Astrovirus (GoAstV) may exacerbate the severity of gout symptoms (He, Wang, Zhao, Jiang, Zhang, Wei, Wu, Wang, Diao and Tang, 2022a; Liu, et al., 2020a). In China, the incidence rate of GPV was reported to reach 12.74 % (251 out of 1970) in 2021 (He, Wang, Zhao, Jiang, Zhang, Wei, Wu, Wang, Diao and Tang, 2022a). Heilongjiang Province serves as a critical region for both the goose industry and the incidence of GPV. Despite its significance, there is a paucity of research on the genetic characteristics of GPV. Furthermore, recent years have witnessed numerous outbreaks of SBDS among mule duck and Cherry Valley duck populations across various regions in China. The etiology of SBDS is attributed to the recombination of GPV, resulting in NGPV strains (He, et al., 2022b). Therefore, the genetic evolution of GPV has once again attracted people's attention. This study isolated one GPV strain from Heilongjiang Province, which is a recombinant strain of the vaccine strain. Moreover, the isolated strain has high homology with some VP3 sequences of duck derived parvovirus, suggesting that GPV is still undergoing evolution and recombination during the transmission of

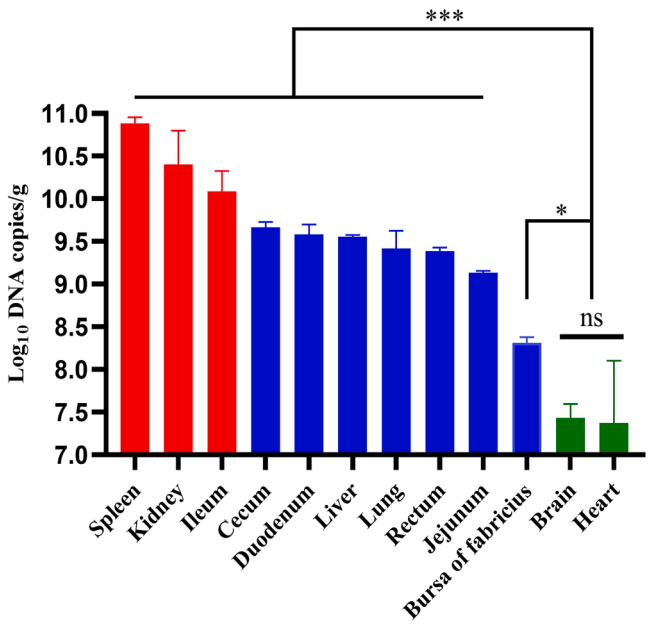

Fig. 7. Virus distribution in HLJ2023-inoculated goslings at 72 hpi. Note: ** indicates that the difference between the infection group and control group was extremely significant.

different species, which should be of concern to researchers.

GPV and MDPV belong to the same genus of dependent parvoviruses, which are small non-enveloping viruses carrying a linear single stranded DNA genome of approximately 5 kb in length. There are two open reading frames (ORFs) in waterfowl parvovirus. The left ORF encodes non-structural (NS) proteins NS1 and NS2, while the right ORF encodes structural proteins VP1, VP2, and VP3 (Wang, et al., 2020; Yang, et al., 2020). Among them, VP3 is the main capsid protein of GPV, accounting for about 80 % of the total capsid protein (Tarasiuk, et al., 2015). It is also the main immune protective antigen of GPV, which can induce the body to produce neutralizing antibodies. Interestingly, SimPlot analysis in this study showed that the VP3 gene exhibited high homology in GPV, NGPV, MDPV and GMD. Compared to GPV, MDPV showed even higher homology in 3519-4219 nt. Therefore, the classical GPV may have a certain protective effect in the prevention and treatment of GPV, NGPV, and MDPV. However, further research is needed to explore the effectiveness of existing GPV vaccines.

"Thrombosis" usually refers to the solid substance formed in blood vessels during the infection process caused by gosling plague virus, which blocks blood vessels and affects blood circulation. Thrombosis is often considered a typical symptom of GPV infection (Niu, et al., 2018b). Significant vascular damage was observed in the dead goslings dissected in this study, while emboli had not yet formed, which may be due to the rapid onset of in the gosling disease and death before embolism formation. Previous reports have shown that the gosling plague virus can invade multiple organs of goslings, including the digestive system, respiratory system, and nervous system (Ning, et al., 2017; Yan, et al., 2019). In this study, goslings may experience symptoms such as diarrhea, difficulty breathing, and nerve reactions such as arches after being infected with GPV. The analysis of viral load in various tissues of infected goslings showed that the intestinal system is the main infection area of the virus. In addition, the presence of the virus was also detected in the heart and brain tissues, with significantly lower viral load than that in the intestine and other tissues. Histopathological analysis of different tissues showed structural abnormalities in the duodenum and jejunum, with columnar epithelium and intestinal glands completely replaced by residual protein fibers. There are varying degrees of tissue damage in liver, lung, and kidney tissues. In recent years, reports have shown that co infection of GPV and GoAstV may lead to more severe symptoms of gout in geese, which may be related to kidney damage in goslings (Liu et al., 2020a). In summary, this study suggests that even if goslings infected with GPV do not form solid emboli, the GPV may still pose a serious threat to their health and life of goslings.

Since 2015, there has been an outbreak of short beaked dwarf syndrome (SBDS) caused by NGPV in China. This infectious disease is widely and rapidly spread in China's duck farms, with a high incidence rate and huge economic losses (Kexiang, Yu, Xiuli, Ma, Zizhang, Sheng, Lihong, Qi, Cunxia and microbiology, 2016). Subsequent reports have shown that this kind of NGPV is derived from the recombination of the classic GPV, which is believed to play a crucial role in the evolution of parvovirus (Kexiang, Yu, Xiuli, Ma, Zizhang, Sheng, Lihong, Qi, Cunxia and microbiology, 2016). Multiple classic GPV strains were involved in the recombination of NGPV. In this study, evolutionary analysis showed a close genetic evolutionary relationship between the isolated strain and the NGPV from ducks. SimPlot analysis showed that the HLJ2023 strain isolated in this study exhibited high homology with MDPV and GMD, which was between 3519 and 4219 nt. Recombinant analysis showed that the strain HLJ2023 isolated in this study may be a potential recombinant strain of the NGPV JS191021 strain and the GMD PT strain (Wang, et al., 2014; Zádori, et al., 1995). These findings suggest the presence of intricate and frequent recombination events within the GPV, underscoring the necessity for heightened caution in the application of live vaccines for waterfowl parvovirus.

In conclusion, this study effectively isolated the GPV HLJ2023 strain from goose tissue with intestinal embolism. The isolated strain is a potential recombinant strain derived from NGPV JS191021 strain and the GMD PT strain, with strong pathogenicity. Furthermore, phylogenetic analysis reveals that VP3 gene shares a close genetic evolutionary relationship with both MDPV and GMD. These findings contribute significantly to our comprehension of the genetic evolutionary traits of avian parvovirus. At the same time, frequent mutations and recombination also indicate the necessity of monitoring the genetic evolution system of avian parvovirus.

Author contributions

Dongbo Sun conceived and designed the experiments; Qinghe Zhu, Huinan Li, Hansong Li, and Wenfei Bai performed the experiments; Jingxuan Zhou, Ming Liu, Yingying Zhao, Limin Jiang, Ying Sun, Jia Sun, Jingjing Zhao, Jia Hu, Chunqiu Li, Xiaoxu Xing and Dan Yang analyzed the data; Dongbo Sun and Qinghe Zhu wrote the paper.

Disclosures

The authors declare that they have no competing interests.

Acknowledgements

This work was supported by the National Funds for Supporting Reform and Development of Heilongjiang Provincial Colleges and Universities (grant no. 2022010009), Science and Technology Planning Project of Daqing City (grant no. zd-2024-29).

Supplementary materials

Supplementary material associated with this article can be found, in the online version, at doi:10.1016/j.psj.2025.105231.

References

Dong, H.X.N., 2011. Establishment and application of Fluorescence quantitative PCR for identification of goose parvovirus. Chin. J. Vet. Drug 9, 4. https://doi.org/10.3969/j.issn.1002-1280.2011.09.006.

Gibbs, M.J., Armstrong, J..S., Gibbs, A.J., 2000. Sister-scanning: a Monte Carlo procedure for assessing signals in recombinant sequences. Bioinformatics 16, 573–582. https://doi.org/10.1093/bioinformatics/16.7.573.

He, D., Wang, F., Zhao, L., Jiang, X., Zhang, S., Wei, F., Wu, B., Wang, Y., Diao, Y., Tang, Y., 2022a. Epidemiological investigation of infectious diseases in geese on mainland China during 2018-2021. Transbound Emerg Dis. 69, 3419–3432. https://doi.org/10.1111/tbed.14699.

He, J., Zhang, Y., Hu, Z., Zhang, L., Shao, G., Xie, Z., Nie, Y., Li, W., Li, Y., Chen, L., Huang, B., Chu, F., Feng, K., Lin, W., Li, H., Chen, W., Zhang, X., Xie, Q., 2022b. Recombinant Muscovy duck parvovirus led to Ileac damage in Muscovy ducklings. Viruses 14, 1471. https://doi.org/10.3390/v14071471.

Huo, X., Chen, Y., Zhu, J., Wang, Y., 2023. Evolution, genetic recombination, and phylogeography of goose parvovirus. Comp. Immunol. Microbiol. Infect. Dis. 102, 102079. https://doi.org/10.1016/j.cimid.2023.102079.

Irvine, R., Ceeraz, V., Cox, B., Twomey, F., Young, S., Bradshaw, J., Featherstone, C., Holmes, J.P., Ainsworth, H., Jones, R., 2008. Goose parvovirus in Great Britain. Vet. Rec. 163, 461. https://doi.org/10.1136/vr.163.15.461.

Jiang, N., Wang, E., Guo, D., Wang, X., Su, M., Kong, F., Yuan, D., Zhai, J., Sun, D., 2018. Isolation and molecular characterization of parainfluenza virus 5 in diarrhea-affected piglets in China. J. Vet. Med. Sci. 80, 590–593. https://doi.org/10.1292/jvms.17-0581.

Kardogan, O., Mustak, H.K., Mustak, I.B., 2020. The first detection and characterization of goose parvovirus (GPV) in Turkey. Trop. Anim. Health Prod. 53, 36. https://doi.org/10.1007/s11250-020-02463-8.

Kexiang, Y.u, X., Ma, Z., Sheng, L., Qi, Cunxia, and L. J. J. o. c. microbiology. 2016. Identification of goose-origin parvovirus as a cause of newly emerging beak atrophy and dwarfism syndrome in ducklings.

Letunic, I., Bork, P., 2016. Interactive tree of life (iTOL) v3: an online tool for the display and annotation of phylogenetic and other trees. Nucleic. Acids. Res. 44, W242–W245. https://doi.org/10.1093/nar/gkw290.

Li, K.P., Hsu, Y..C., Lin, C.A., Chang, P.C., Shien, J.H., Liu, H.Y., Yen, H., Ou, S.C., 2021. Molecular characterization and pathogenicity of the novel recombinant Muscovy Duck parvovirus isolated from geese. Anim. (Basel) 11, 3211. https://doi.org/10.3390/ani11113211.

Liu, H., Hu, D., Zhu, Y., Xiong, H., Lv, X., Wei, C., Liu, M., Yin, D., He, C., Qi, K., Wang, G., 2020a. Coinfection of parvovirus and astrovirus in gout-affected goslings. Transbound Emerg Dis. 67, 2830–2838. https://doi.org/10.1111/tbed.13652.

Liu, J., Su, X., Wang, Z., Qin, J., 2018. Isolation and identification of Goose plague virus in Guangdong region and analysis of whole gene sequence. Chin. J. Vet. Med. 54, 5.

Liu, P., J. Zhang, S. Chen, M. Wang, and A. J. G. A. Cheng. 2017. Genome sequence of a goose parvovirus strain isolated from an ill goose in China. 5:e00227-00217.

Liu, W.J., .Y. T. Yang, H.Y. Zou, S.J. Chen, C. Yang, Y. B. Tian, and Y.M.J.V.g. Huang. 2020b. Identification of recombination in novel goose parvovirus isolated from domesticated Jing-Xi partridge ducks in South China. 56:600-609.

Martin, D.P., Murrell, B.., Golden, M., Khoosal, A., Muhire, B., 2015. RDP4: detection and analysis of recombination patterns in virus genomes. Virus Evol. 1, vev003. https://doi.org/10.1093/ve/vev003.

Martin, D.P., Posada, D.., Crandall, K.A., Williamson, C., 2005. A modified bootscan algorithm for automated identification of recombinant sequences and recombination breakpoints. AIDS Res. Hum. Retroviruses 21, 98–102. https://doi.org/10.1089/aid.2005.21.98.

Ning, K., Wang, M., Qu, S., Lv, J., Yang, L., Zhang, D., 2017. Pathogenicity of Pekin duck- and goose-origin parvoviruses in Pekin ducklings. Vet. Microbiol. 210, 17–23. https://doi.org/10.1016/j.vetmic.2017.08.020.

Niu, X., Wang, H., Wei, L., Zhang, M., Yang, J., Chen, H., Tang, Y., Diao, Y., 2018a. Epidemiological investigation of H9 avian influenza virus, Newcastle disease virus, Tembusu virus, goose parvovirus and goose circovirus infection of geese in China. Transbound Emerg. Dis. 65, e304–e316. https://doi.org/10.1111/tbed.12755.

Niu, Y., Zhao, L., Liu, B., Liu, J., Yang, F., Yin, H., Huo, H., Chen, H., 2018b. Comparative genetic analysis and pathological characteristics of goose parvovirus isolated in Heilongjiang, China. Virol. J. 15, 27. https://doi.org/10.1186/s12985-018-0935-5.

Padidam, M., Sawyer, S., Fauquet, C.M., 1999. Possible emergence of new geminiviruses by frequent recombination. Virology 265, 218–225. https://doi.org/10.1006/viro.1999.0056.

Posada, D., Crandall, K.A., 2001. Evaluation of methods for detecting recombination from DNA sequences: computer simulations. Proc. Natl. Acad. Sci. U. S. A. 98, 13757–13762. https://doi.org/10.1073/pnas.241370698.

Qi, S., Su, M., Guo, D., Li, C., Wei, S., Feng, L., Sun, D., 2019. Molecular detection and phylogenetic analysis of porcine circovirus type 3 in 21 provinces of China during 2015-2017. Transbound Emerg. Dis. 66, 1004–1015. https://doi.org/10.1111/tbed.13125.

Smith, J.M., 1992. Analyzing the mosaic structure of genes. J. Mol. Evol. 34, 126–129. https://doi.org/10.1007/BF00182389.

Tamura, K., Stecher, G., Peterson, D., Filipski, A., Kumar, S., 2013. MEGA6: molecular Evolutionary Genetics Analysis version 6.0. Mol. Biol. 30, 2725–2729. https://doi.org/10.1093/molbev/mst197.

Tarasiuk, K., Wozniakowski, G., Holec-Gasior, L., 2015. Expression of goose parvovirus whole VP3 protein and its epitopes in Escherichia coli cells. Pol. J. Vet. Sci. 18, 879–880. https://doi.org/10.1515/pjvs-2015-0114.

Tatar-Kis, T., Mato, T., Markos, B., Palya, V., 2004. Phylogenetic analysis of Hungarian goose parvovirus isolates and vaccine strains. Avian. Pathol. 33, 438–444. https://doi.org/10.1080/03079450410001724067.

Wang, J., Duan, J., Meng, X., Gong, J., Jiang, Z., Zhu, G., 2014. Cloning of the genome of a goose parvovirus vaccine strain SYG61v and rescue of infectious virions from recombinant plasmid in embryonated goose eggs. J. Virol. 200, 41–46. https://doi.org/10.1016/j.jviromet.2014.02.014.

Wang, J., Li, W., Gong, X., Wang, Z., Wang, Y., Ling, J., Jiang, Z., Zhu, G., Li, Y., 2024. Recombination and amino acid point mutations in VP3 exhibit a synergistic effect on increased virulence of rMDPV. Virulence 15, 2366874. https://doi.org/10.1080/21505594.2024.2366874.

Wang, J., Wang, Z., Jia, J., Ling, J., Mi, Q., Zhu, G., 2019. Retrospective investigation and molecular characteristics of the recombinant Muscovy duck parvovirus circulating in Muscovy duck flocks in China. Avian. Pathol. 48, 343–351. https://doi.org/10.1080/03079457.2019.1605145.

Wang, Y., Cui, Y., Li, Y., Jiang, S., Liu, H., Wang, J., Li, Y., 2020. Simultaneous detection of duck circovirus and novel goose parvovirus via SYBR green I-based duplex real-time polymerase chain reaction analysis. Mol. Cell 53, 101648. https://doi.org/10.1016/j.mcp.2020.101648.

Wang, Y., Sun, J., Zhang, D., Guo, X., Shen, W., Li, Y., 2021. Genetic characterization and phylogenetic analysis of duck-derived waterfowl parvovirus in Anhui province, eastern China. Arch. Virol. 166, 2011–2016. https://doi.org/10.1007/s00705-021-05110-1.

Yan, Y.Q., He, T..Q., Li, R., Zhang, S.Y., Wang, K., Yi, S.S., Niu, J.T., Dong, H., Hu, G.X., 2019. Molecular characterization and comparative pathogenicity of goose parvovirus isolated from Jilin Province, Northeast China. Avian. Dis. 63, 481–485. https://doi.org/10.1637/aviandiseases-D-19-00075.

Yang, Y., Sui, N., Zhang, R., Lan, J., Li, P., Lian, C., Li, H., Xie, Z., Jiang, S., 2020. Coinfection of novel goose parvovirus-associated virus and duck circovirus in feather sacs of Cherry Valley ducks with feather shedding syndrome. Poult. Sci. 99, 4227–4234. https://doi.org/10.1016/j.psj.2020.05.013.

Yin, X., Zhang, S., Gao, Y., Li, J., Tan, S., Liu, H., Wu, X., Chen, Y., Liu, M., Zhang, Y., 2012. Characterization of monoclonal antibodies against waterfowl parvoviruses VP3 protein. Virol. J. 9, 288. https://doi.org/10.1186/1743-422X-9-288.

Zádori, Z., R. Stefancsik, T. Rauch, and J. K. J. Virology. 1995. Analysis of the complete nucleotide sequences of goose and muscovy duck pervoviruses indicates common ancestral origin with Adeno-associated virus 2. 212:562-573.